The Saxitoxin/Tetrodotoxin Binding Site on Cloned Rat Brain IIa Na Channels is in the Transmembrane Electric Field

Jonathan Satin, James T. Limberis, John W. Kyle, Richard B. Rogart, and Harry A. Fozzard
Cardiac Electrophysiology Labs, Departments of Medicine and the Pharmacological and Physiological Sciences and the Committee on Cell Physiology, The University of Chicago, Chicago, Illinois 60637 USA

ABSTRACT The rat brain IIa (BrIIa) Na channel α-subunit and the brain β1 subunit were coexpressed in *Xenopus* oocytes, and peak whole-oocyte Na current (I_{Na}) was measured at a test potential of −10 mV. Hyperpolarization of the holding potential resulted in an increased affinity of STX and TTX rested-state block of BrIIa Na channels. The apparent half-block concentration (ED_{50}) for STX of BrIIa current decreased with hyperpolarizing holding potentials (V_{hold}). At V_{hold} of −100 mV, the ED_{50} was 2.1 ± 0.4 nM, and the affinity increased to a ED_{50} of 1.2 ± 0.2 nM with V_{hold} of −140 mV. In the absence of toxin, the peak current amplitude was the same for all potentials negative to −90 mV, demonstrating that all of the channels were in a closed conformation and maximally available to open in this range of holding potentials. The Woodhull model (1973) was used to describe the increase of the STX ED_{50} as a function of holding potential. The equivalent electrical distance of block (δ) by STX was 0.18 from the extracellular milieu when the valence of STX was fixed to +2. Analysis of the holding potential dependence of TTX block yielded a similar δ when the valence of TTX was fixed to +1. We conclude that the guanidinium toxin site is located partially within the transmembrane electric field. Previous site-directed mutagenesis studies demonstrated that an isoform-specific phenylalanine in the BrIIa channel is critical for high affinity toxin block. Therefore, we propose that amino acids at positions corresponding to this Phe in the BrIIa channel, which lie in the outer vestibule of the channel adjacent to the pore entrance, are partially in the transmembrane potential drop.

INTRODUCTION

Mutation studies of the Na channel α-subunit have identified residues that are essential for guanidinium toxin block (Noda et al., 1989). Mutations in the SS2 segment of the S5-S6 loops (Guy and Conti, 1990) of the four Na channel repeat regions also alter single channel conductance (Terlau et al., 1991), confirming that the toxins block in or near the channel's ion conduction path. Na channel isoforms also show marked different sensitivity to toxin block resulting from sequence differences in the toxin binding region of the ion conduction path (Satin et al., 1992a; Heinemann et al., 1992; Backx et al., 1992).

Divalent cations block within the open channel, and they also compete with toxin binding to the channel, with isoform-specific differences in the blocking affinity and competitive efficacy (Schild and Moczydlowski, 1991; Doyle et al., 1993). Mutations affecting toxin affinity simultaneously change the divalent ion blocking affinity (Pusch et al, 1991; Heinemann et al., 1992; Backx et al., 1992), implying that the divalent ion-blocking site and the guanidinium-binding site overlap each other. Analysis of the voltage dependence of Ca, Cd, and Zn block has revealed binding sites that are 15–20% into the membrane field (Yamamoto et al., 1984;Nilius, 1988; Sheets et al., 1987; Backx et al., 1992). If this divalent cation blocking site and the toxin site overlap, then the toxin binding site should be within the transmembrane potential drop (Doyle et al., 1993; Backx et al., 1992).

Initial studies of guanidinium toxin block of BTX-treated brain Na channels in artificial lipid bilayers showed substantial voltage dependence, as if the toxins were bound 50–75% through the transmembrane potential gradient (French et al., 1984; Moczydlowski et al., 1984; Green et al., 1987a). This voltage dependence has been attributed to conformation-dependent differences in binding affinity rather than to a binding site within the transmembrane potential drop, because the voltage dependence is the same for the divalent STX and for the monovalent TTX (Worley and Krueger, 1984; Rando and Strichartz, 1986). These conformation-dependent differences in toxin affinity (Cohen et al., 1981; Salgado et al., 1986; Lönnendonker, 1989) complicate the measurement of the equivalent electrical distance of toxin block.

We have reexamined the question of voltage-dependence of TTX and STX block by studying the effects of hyperpolarization on rested-state block in cloned rat brain and cardiac Na channels in a voltage range where conformational changes are limited. These channels expressed in *Xenopus* oocytes have a shift of kinetic parameters in the depolarizing direction relative to native channels, so that the studies could be performed without significant binding to the open or the inactivated states of the channel. We found that blocking efficacies for both toxins were increased by hyperpolarization. The voltage dependence of the divalent STX was

Received for publication 6 December 1993 and in final form 10 June 1994.
Address reprint requests to Jonathan Satin, Ph.D., Cardiac Electrophysiology Labs., MC-6094, University of Chicago, 5841 S. Maryland Ave., Chicago, IL 60637. Tel.: 312-702-4447; Fax: 312-702-6789; E-mail: satin@hearts.bsd.uchicago.edu.

0006-3495/94/09/1007/08 $2.00

greater than that of monovalent TTX, but when we adjusted for the difference in valence, both toxins appeared to block approximately 15% into the transmembrane potential gradient. This electrical distance is similar to that of divalent ion block, supporting the conclusion that both toxins and divalent ions are affected by the transmembrane potential drop and block at overlapping sites.

MATERIALS AND METHODS

Xenopus oocytes were injected with cRNA and clamped with the two-electrode method as previously described (Satin et al., 1992b). Oocytes were injected with 10–50 ng of cRNA. One to ten days after injection, oocytes were impaled and whole-oocyte currents were recorded in a flowing bath solution containing (in mM): 90 NaCl, 2.5 KCl, 1 $CaCl_2$, 1 $MgCl_2$, 10 HEPES (pH 7.6). The bath volume was less than 500 μl. Oocytes expressing >5 μA of I_{Na} were generally not useful because V_m was not stable at the time of the peak current. A two electrode voltage clamp/bath clamp (Dagan model CA-1) was used to measure Na currents in oocytes. To improve clamp speed, electrode resistances were usually less than 1 MΩ (range from 0.2 to 1 MΩ). Capacitive transients were not subtracted because the large membrane area of the oocyte (diameter ~1 mm) resulted in a transient that saturated the recording system. Leak currents were not subtracted because at −10 mV the leak was negligible compared with the expressed current. We never detected an endogenous oocyte Na current.

Both V_m and current were recorded. V_m was measured as the difference between a voltage-recording electrode in the bath and the voltage-sensing electrode impaled in the oocyte. Only oocytes clamped to the command potential at the time of peak current were used for data analysis. Initial toxin-free and washout controls were performed on most oocytes for the dose response curves. Only stable oocyte impalements were used for data analysis. Between the initial toxin-free recording and final washout the holding current at V_{hold} = −100 mV increased by an average of −13 ± 42 nA (n = 11). Peak current levels in washout controls for a V_{test} of −10 mV ranged from 91 to 104% of the initial controls. Dose response curves for individual cells were fitted, and the ED_{50} values are reported as the mean ± SD. Significant differences were tested using a two-sample t-test.

The brain β1 subunit was cloned from a rat brain cDNA library using PCR. A 28 base forward primer was synthesized corresponding to base pair 201–228 (Isom et al., 1992; 5′-cccaccgccttgcgcggcgccatggggacg-3′). Further details are presented in Satin et al. (1994). The DNA sequence exactly corresponded to that reported by Isom et al. (1992).

RESULTS

Fig. 1 shows Na currents elicited by a voltage step from a holding potential (V_{hold}) of −140 and −100 mV to a test potential of −10 mV in oocytes expressing BrIIa + β1. Changing V_{hold} from −100 to −140 mV had no effect on the amplitude of the peak current in the absence of toxin (Fig. 1, *A* and *B*). The final toxin washout current traces are superimposed on the initial toxin-free currents. Throughout this study, we observed less than a 10% change in peak current amplitude between the initial toxin-free control and the final toxin washout.

At pH 7.6, STX has a net valence of +2. If the block of Na channels by STX occurs within the transmembrane-voltage drop, then block should occur with higher affinity at hyperpolarized potentials. In the presence of 3 nM STX, peak I_{Na} during the test pulse is reduced after a V_{hold} of −140 mV compared with a V_{hold} of −100 mV (Fig. 1, *C* and *D*). The

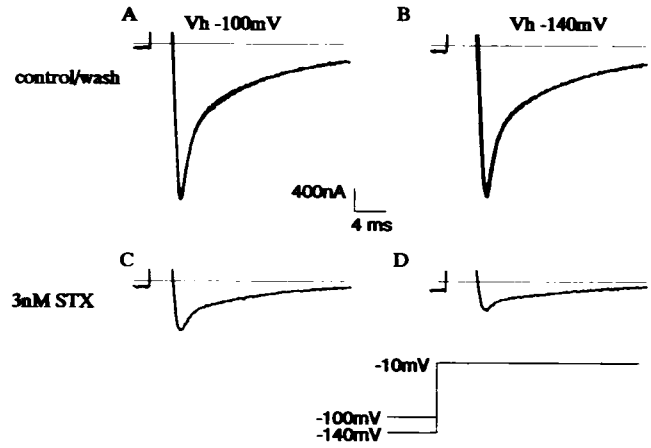

FIGURE 1 Effect of holding potential on STX block of Na currents expressed from BrIIa + β1 in *Xenopus* oocytes. Na current (I_{Na}) were recorded during steps to −10 mV after holding potentials (V_{hold}) of either −100 mV (*A*, *C*) or −140 mV (*B*, *D*). (*A*, *B*) Current traces for initial toxin-free control and washout of toxin are superimposed. In the absence of toxin, the peak amplitude of current was the same for all V_{hold} values in range from −140 to −100 mV. (*C*, *D*) 3 nM STX blocks less current after a V_{hold} of −100 mV (*C*; 67% block) than after −140 mV (*D*; 81% block). V_{hold} was maintained for at least 90 s. The dashed line is the zero current level. Cell z30322B.

block by STX shown in Fig. 1 represents tonic block, defined as that which occurs after infrequent stimulation. In these experiments, V_{hold} was maintained for at least 90 s in the presence of STX. Dose response curves for BrIIa + β1 and RHI from V_{hold} −140, −120, and −100 mV are presented in Fig. 2, *A* and *B*. Peak current after 30 s at V_{hold} were normalized to the peak current in the absence of STX. The fitted ED_{50} from a single site dose response curve is reduced as V_{hold} is made more negative for both BrIIa + β1 and RHI.

The dependence of ED_{50} on V_{hold} can be described by a transmembrane voltage effect on STX block. Fig. 3 is the fitted ED_{50} plotted as a function of V_{hold}. The line is a fit to the Woodhull model (1973) for voltage-dependent block of the form:

$$ED_{50}(V) = ED_{50}(0) * \exp[\delta * z * V_{hold} * (e/kT)], \quad (1)$$

where $ED_{50}(0)$ is the extrapolated half-block concentration at 0 mV, δ is the equivalent electrical distance (from the outside), z is the valence of the blocker, and e, k, and T have their usual meanings. The δ values calculated for STX block of BrIIa + β1 (0.18 ± 0.02, n = 5) and RHI (0.14 ± 0.05, n = 3) assuming a valence of +2 for STX are only slightly different (p = 0.09). This suggests that the STX site for BrIIa and RHI channels is located in a similar position with respect to the electrical field. The ED_{50}(−100 mV) for BrIIa + β1 (2.1 ± 0.4 nM) is 51 times more sensitive to STX than that for RHI (107 ± 9 nM).

The simplest model for voltage-dependent block is that blocking efficacy is affected because the charged blocker is influenced by the transmembrane potential drop. At the bulk solution pH of 7.6, STX is primarily +2 and should have

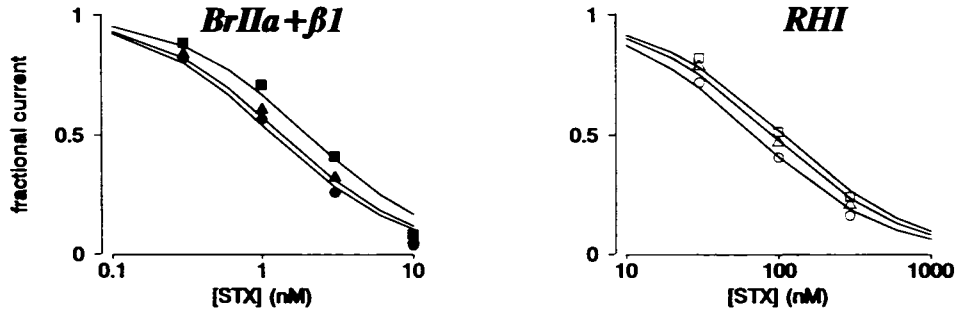

FIGURE 2 STX blocks with a higher affinity at more hyperpolarized holding potentials. Dose response curves at V_{hold} −100, −120, and −140 mV for BrIIa + β1 (*A*) and RHI (*B*). Individual oocytes were fitted to single site dose response curve of the form

$$I_{Na,STX/Na,CONTROL} = (1 + ED_{50}/[STX])^{-1}, \quad (5)$$

where ED_{50} represents the half-block concentration of I_{Na} by STX. The solid line is the average of the fitted ED_{50} values from individual cells. The fitted ED_{50} is reduced by hyperpolarization. For BrIIa + β1, the ED_{50} values are: 2.1 ± 0.4, 1.4 ± 0.2, and 1.2 ± 0.2 nM (n = 5 oocytes) at −100, −120, and −140 mV, respectively; for RHI, the ED_{50} values are: 107 ± 9, 91 ± 8, and 69 ± 9 nM (n = 3 oocytes) at −100, −120, and −140 mV, respectively. *Squares*, *triangles*, and *circles* represent V_{hold} = −100, −120, and −140 mV, respectively.

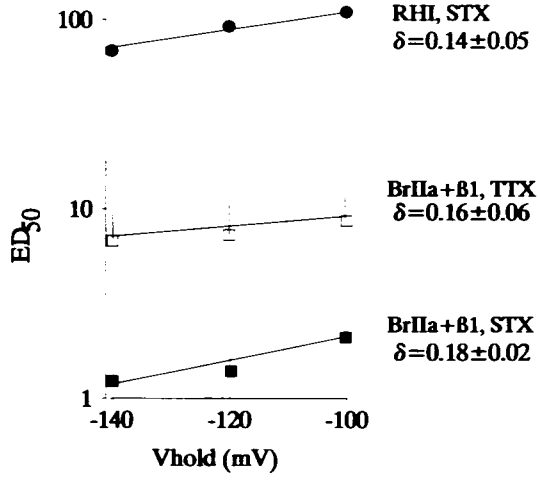

FIGURE 3 Analysis of voltage dependence of toxin block according to the Woodhull method (——). Fitted STX ED_{50} (from Fig. 2) for BrII + β1 and RHI plotted as a function of V_{hold}. TTX ED_{50} is also plotted as a function of V_{hold} for BrIIa + β1. The valence of STX was fixed to +2 and TTX +1 for the fit to the data. Transmembrane voltage-dependent block requires that the calculated electric distance (δ) for +1 TTX is the same as +2 STX. The fitted δ for BrIIa + β1 block by STX was 0.18 ± 0.02 and by TTX was 0.20 ± 0.07. For BrIIa + β1 the 0 mV ED_{50} was 8.9 ± 3.0 nM for STX and 24 ± 8 nM for TTX. For RHI δ = 0.14 ± 0.05 and $ED_{50}(0)$ = 333 ± 103 nM. The solid line is the mean of the fitted parameters from individual oocytes.

more of an effect than TTX, which is +1 at this pH. If the toxin block site is within the transmembrane potential gradient, and if the increased block with the more negative V_{hold} is not caused by a conformational change, then the calculated equivalent electrical distance, δ, should be similar for TTX and STX. The δ calculated for TTX block, assuming a valence of +1, was 0.16 ± 0.06 (n = 6); this is not significantly different (t-test, $p > 0.1$) from the δ of STX block (z = +2) of BrIIa. This result suggests that the site for rested state block is within the transmembrane potential drop.

The assumption that no significant conformational changes occur in the voltage range from V_{hold} of −100 to −140 mV was examined by steady-state availability curves. The availability curve for BrIIa + β1 (Fig. 4) demonstrates that after a 10 s conditioning potential step (V_{cond}) at −90 mV channels are maximally available to open upon depolarization in the absence of toxin (Fig. 4, *squares*). The midpoints of the curves in the presence of toxin are shifted about −5 mV in the hyperpolarizing direction. We can attribute this shift in the voltage range of −90 to −40 mV to a maintained inactivated state block of Na channels (Carmeliet, 1987; Eickhorn et al., 1990) and we did not consider this effect further. Peak currents are normalized to V_{cond} = −90 mV to illustrate this shift (Fig. 4 *B*). In the range of the fully available limb of the curves in Fig. 4 (−140 to −90 mV), additional toxin block is obtained as the conditioning potential is made more negative. The steady-state block curves for control (*squares*), 3 nM STX (*circles*), and 30 nM TTX (*triangles*) are superimposed. 3 nM STX and 30 nM TTX cause greater than 50% block of current (Fig. 4 *A*). Negative to −90 mV, channels are maximally available to open, and the fraction of blocked channels in this range can be described by

$$y(V) = \left(1 + \frac{ED_{50}(V)}{[\text{toxin}]}\right)^{-1}, \quad (2)$$

where $y(V)$ is the fraction of blocked channels as a function of potential, and $ED_{50}(V)$ is the concentration of toxin for half-block of I_{Na} (Eq. 1). The product of valence and electrical distance ($z\delta$, the effective valence) was twice as large for STX (0.28 ± 0.05; n = 7) as for TTX (0.13 ± 0.04; n = 4), and the δ values are not significantly different. Assuming a valence of +2 for STX and +1 for TTX, both toxins block at the same equivalent electrical distance.

Although the I_{Na} was fully available at potentials of −90 mV and more negative, there are likely to be alterations in the equilibrium between different closed states, the so called

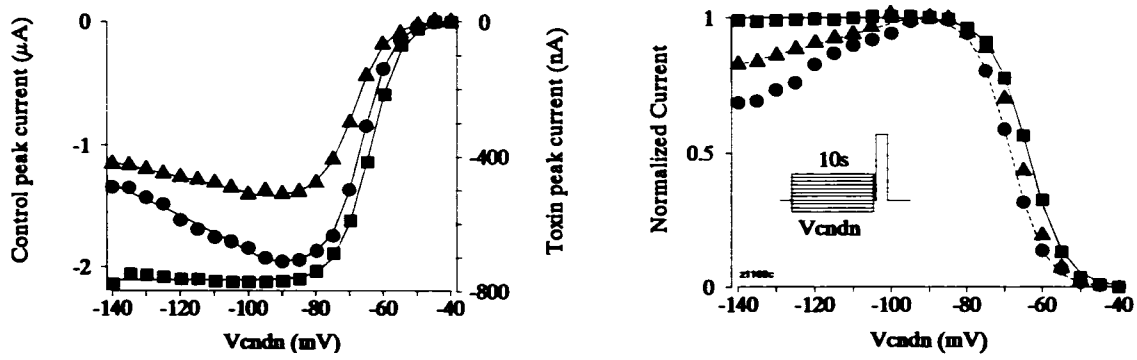

FIGURE 4 STX and TTX block at the same equivalent electrical distance. Steady-state availability curves for control (■, ——), 30 nM TTX (▲, – – –), and 3 nM STX (●, - - - -) in the same cell are superimposed. (*A*) Peak current amplitudes are plotted as a function of the conditioning potential (V_{condn}). Negative to −90 mV channels are fully available to open in the absence of toxin. In the presence of toxin the lines negative to V_{condn} = −90 mV are the data fit to Eq. 3 (see text). For this cell δ = 0.14 and 0.13 for STX and TTX, and ED_{50}(0 mV) = 4 and 16 nM for STX and TTX, respectively. Positive to −90 mV the solid line is a Boltzmann fit to an availability curve of the form:

$$I_{Na,max} = (1 + \exp[(Vcondn - V_{1/})/k])^{-1}, \quad (6)$$

where $V_{1/2}$ is the midpoint and k is the slope. $V_{1/2}$ was −64 mV in control, −66 in 3 nM STX, and −68 in the presence of 30 nM TTX. k (=5) was unchanged in the presence of toxin. (*B*) Peak current amplitudes were normalized to the peak current at V_{condn} = −90 mV. The conditioning pulse duration was 10 s. cell z31103c.

Cole-Moore shift (Cole and Moore, 1960; Taylor and Bezanilla, 1983). Therefore, we performed an additional test that is necessary to prove that STX block in the fully available voltage range is caused by a transmembrane potential effect. The STX association rate is two orders of magnitude slower than a diffusion limited process, and is on the order of 10^7 M^{-1} s^{-1} (Ulbricht, 1986; Guo et al., 1987). For concentrations used for BrIIa + β1, we predict that we need to maintain a constant voltage for several seconds to reach a new equilibrium for STX block. The raw current traces superimposed in the left panel of Fig. 5 correspond to current elicited by depolarizations from a 10s long V_{condn} of either −140 (*A* and *D*) or −100 mV (*B* and *C*). The 10 s V_{cond}-dependent block by 10 nM STX is shown in traces *C* and *D*. The dashed line in the right panel of Fig. 5 (*open triangles*) represents the current measured in the presence of 10 nM STX after conditioning pulses of only 100 ms. Presumably, a conditioning potential step (V_{cond}) for 100 ms did not allow voltage-dependent changes in block to occur, whereas a 10 s V_{cond} in the same cell resulted in additional block with a δ = 0.17 (compare traces *C* and *D*). This suggests that if a conformational change is responsible for changes in toxin block in the hyperpolarized range of potentials, it must develop with time constants of several seconds. The time course of this additional block is more appropriate to the expected toxin binding rate than to state-dependent changes.

Because toxin takes seconds to reach voltage-dependent steady-state block levels the fraction of V_{hold}-dependent block should be independent of V_{test}. We measured the fraction of

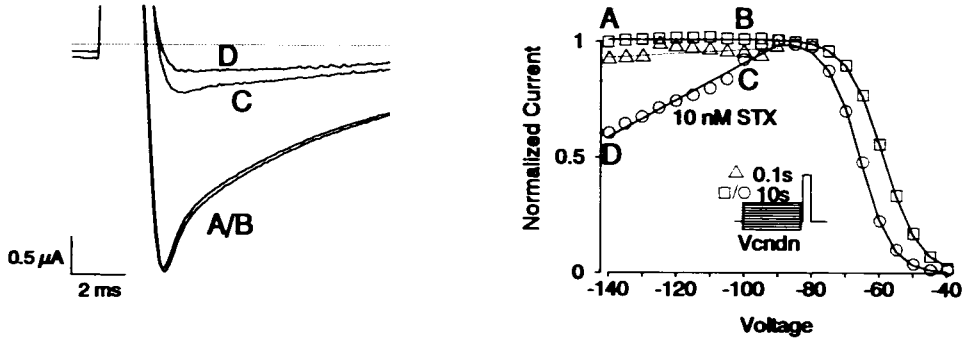

FIGURE 5 Steady-state availability of BrIIa + β1 in the absence and presence of 10 nm STX. Channels are maximally available to open after a 10 s conditioning step to potentials negative to −90 mV in the absence of toxin (□). (*left*) Current traces in absence of toxin show no effect on V_{condn} of −100 or −140 mV (traces *A* and *B*, respectively). Traces *C* and *D* are recorded in the presence of 10 nM STX. More current was present after 10 s at −100 (trace *C*) than at −140 mV (trace *D*). (*right*) For hyperpolarized conditioning potentials (<−90 mV) of 10-s duration, the peak current was progressively less in the presence of 10 nM STX (○). This voltage-dependent block of current was dependent on the duration of the conditioning potential (V_{condn}). The dashed line is drawn through the normalized current after a 100-ms V_{condn}. Only a slight diminution of peak current is observed after a 100-ms V_{condn} at hyperpolarized potentials. In the presence of 10 nM STX the slope, k, was the same, but the $V_{1/2}$ was shifted −6 mV relative to control. Peak current amplitudes were normalized to the peak current at V_{condn} = −90 mV. Cell z30119A.

block as a function of V_{hold} using V_{test} ranging from −20 to +10 mV in the linear phase of the current-voltage curve. 90 s was maintained between voltage steps to allow steady-state conditions to develop. Varying V_{test} had no effect on the degree of V_{hold}-dependent block by STX.

Estimation of the rates of development and relief of voltage-dependent block

Hyperpolarization of the holding potential from −100 to −140 mV for 10 s (Fig. 4) or 90 s (Figs. 1 and 2) increased the affinity of tonic STX and TTX block. To estimate the rate of development of this extra block induced by negative potentials, we held the membrane potential at −140 mV for variable durations before stepping to a test pulse. This protocol has no effect on the amplitude of toxin free current (Fig. 6 *A*). Fig. 6 *B* shows the time course of development of field effect block of BrIIa + β1 by 1 and 3 nM STX. Development of field effect block is fit with a single exponential. The rate of development (from the single exponential fit) of field effect block by STX increases with dose. If the rate of development of block is a function of STX concentration, then it should be fit with a straight line (Fig. 6 *C*). If we assume a first order reaction scheme such that

$$\text{STX} + \text{Channed} \leftrightarrows \text{STX} \cdot \text{Channel} \qquad (3)$$

then

$$1/\tau_{on} = K_{off} + K_{on} * [\text{STX}]. \qquad (4)$$

The fit to this equation in Fig. 6 *C* yields a K_{on} of $63 \cdot 10^6$ M^{-1} s^{-1} and a K_{off} of 0.24 s^{-1} at −140 mV for field effect block by STX (n = 15 cells pooled). These values are similar to previously reported values for STX association and dissociation rates for neuronal Na channels (Ulbricht et al., 1986; Satin et al., 1994).

DISCUSSION

The main conclusion of this study is that STX and TTX appear to block the Na channel at a site that is partially within the transmembrane potential gradient. We favor this interpretation over the alternative of state-dependent changes in affinity for the following reasons. 1) The voltage-dependent change in blocking efficacy occurs over a voltage range where the channel is fully available, avoiding the well demonstrated changes in affinity to the inactivated state (e.g., Cohen et al., 1981). 2) The time course of development and relief of this voltage-dependent toxin block is slow and is similar to rate constants measured with radiolabeled toxins, rather than those more rapid rates expected from gating changes. 3) The effective valence ($z\delta$) of STX is about twice as large as that of TTX. 4) The extent of voltage dependence is similar to that of cations that are thought to block within the channel's transmembrane potential gradient and that compete with radiolabeled toxin for binding.

Voltage- versus state dependence of toxin block

The effect of membrane electric potential drop on guanidinium toxin block has been difficult to demonstrate because voltage-dependent gating states are associated with different apparent affinities. These state related types of block include: 1) rested state, or tonic block; 2) maintained inactivated state block (possibly more than one conformation); and 3) activated state block, also referred to as post-repolarization phasic block (Makielski et al., 1993). In this study, we measured voltage-dependent block of rested, or closed state channels. We emphasize that the voltage-dependent block measured in this study is different from use-dependent block (indirectly voltage-dependent) measured after depolarizations that are sufficiently long to accumulate inactivated state blocked channels (Carmeliet, 1987; Cohen et al., 1981; Vassilev et al., 1986). The third type of block, which is use-dependent but does not involve inactivated channels, was more recently

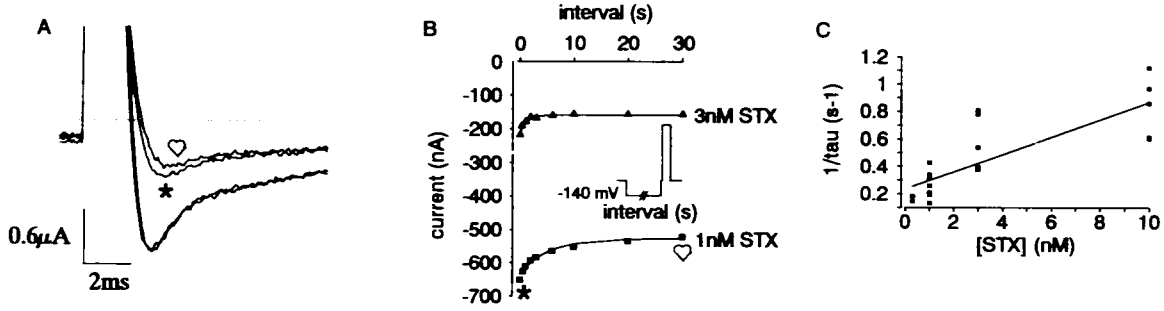

FIGURE 6 The rate of development of STX block at −140 mV. (*A*) Current traces for toxin-free control from V_{hold} −100, stepped to −140 mV for a variable duration, and to a V_{test} of −10 mV. Largest amplitude currents show no dependence on the duration at −140 mV in the absence of toxin. Current traces recorded after a 100 ms and 30 s long hyperpolarization to −140 mV. In the presence of 1 nM STX, more current is measured after a 100-ms hyperpolarization to −140 mV (*) than for a 30 s long hyperpolarization (*polygon*). (*B*) Representative peak current amplitudes plotted as a function of the time interval available for transmembrane voltage drop block to develop at −140 mV. Solid lines are single exponential fits for this cell (cell z30428D). (*C*) The rate of development of block (fitted parameter from panel *A*) vs. [STX] is fit with a straight where the slope represents the association rate constant (K_{on}), and the y intercept is the dissociation rate (K_{off}). The pooled fitted data yielded a $K_{on} = 6.3 \times 10^6$ M^{-1} s^{-1} and $K_{off} = 0.24$ s^{-1} (19 values obtained from 15 cells).

discovered in crayfish axons (Salgado et al., 1986) and was later described in native cardiac (Makielski et al., 1993) and neuronal preparations (Lonnendonker, 1989), and in BrIIa (Patton and Goldin, 1991) and RHI expressed in oocytes (Satin et al., 1994). This latter type of block is elicited after brief depolarizations and is observed after relatively long sojourns in a transiently available state that occurs during recovery from inactivation.

If the guanidinium moiety of TTX or STX binds within the pore, then it was reasoned that the TTX/STX binding site might be within the transmembrane electric field (Hille, 1975; reviewed by Hille, 1992). Subsequent studies of batrachotoxin-treated Na channels showed, however, that association and dissociation rates of guanidinium toxin block was not correlated with the valence of toxin (French et al., 1984; Moczydlowski et al., 1984). This led to the conclusion that the voltage dependence of block was indirect, and was mediated by a voltage dependent conformational change of the channel. In the range of potentials tested in these previous studies, we too observe an apparent increase in block affinity. Specifically, for maintained depolarized potentials we observe an apparent parallel shift of the availability curve to the hyperpolarizing direction in the presence of toxin (Figs. 4 and 5). We interpret this to be caused by a higher affinity, inactivated state block of the channel, or a slowing of the kinetics of recovery from this inactivated state (Eickhorn et al., 1990; Carmeliet, 1987). By the use of maintained hyperpolarized potentials (with only brief, infrequent test depolarizations) and coexpression of the $\beta 1$ subunit with BrIIa, we can minimize entrance of channels into a maintained inactivated state. Peak Na current in whole-oocyte clamp occurs in about 2 ms, so that the degree of block in these experiments reflects only block from toxin binding at V_{hold} and is unrelated to the potential used to elicit Na current.

This ehanced blocking efficacy with hyperpolarization has been described before. Eickhorn and colleagues (1990) also observed TTX block induced by extreme hyperpolarized potentials in cardiac myocytes, but they were unable to quantify their data in this range because of inability to control the voltage in cells at very negative potentials. Channels expressed in oocytes provided advantages over native cell preparations for studying toxin block. In comparison with native channels, the general property of the depolarized shift of the voltage dependence of cloned channels expressed in oocytes (Satin et al., 1992b) allowed us to maintain holding potentials as much as 100 mV negative to the midpoint of the availability curve. Given the relatively slow rates of change of block, the increased block at more negative V_{hold} values appears to be only a function of V_{hold}. At such negative potentials, we assume that no conformational transitions of the channel occur that can affect toxin block. Therefore, we conclude that the increased affinity for STX and TTX block with hyperpolarization is most consistent with a blocking site within the transmembrane potential drop.

Implications of toxin voltage dependence for channel structure

The well known competition between protons and divalent ions and guanidinium toxins for binding to the Na channel suggests overlapping sites of interaction (Doyle et al., 1993). Because the proton block (Woodhull, 1973; Daumas and Andersen, 1993) and divalent ion block (Krueger et al., 1986; Green et al., 1987b; Ravindran et al., 1991; Sheets and Hanck, 1992) are about 20% into the transmembrane voltage drop of the open channel, it was reasonable to think that the toxin binding site might also be within the transmembrane electric field. Point mutations of the SS2 region of the S5-S6 loop of repeat I simultaneously produced changes in toxin binding and in single channel conductance, identifying a four-amino-acid stretch as the toxin binding site and also as part of the ion conduction path (Terlau et al., 1991). Isoform differences in that four-amino-acid stretch influence the toxin affinity and simultaneously the affinity for voltage-dependent divalent ion block. Specifically, the cardiac isoform has a cysteine in position 385 (using the BrIIa numbering system) and it has a low affinity for toxin but a high affinity for Cd^{2+} block. The brain IIa isoform has a phenylalanine in position 385, and it has a high affinity for toxin and a low affinity for Cd^{2+} block. Swap of these residues converts these isoform characteristics (Satin et al., 1992a). The comparable experiment on the skeletal muscle isoform also indicates that the toxin and divalent ion blocking sites include a residue at the same position (Backx et al., 1992). If the divalent ion blocking site is 20% into the transmembrane potential gradient, then the toxin site should also be within the potential gradient to a similar extent. Exact agreement of the fraction of electrical distance would not be expected because the divalent cation and toxin sites are not identical and because the large toxin molecule might not be considered equivalent to a point charge. Nevertheless, these experiments indicate that toxin binding is influenced by about 15% of the electric field of the closed channel, provided that the measurements are done in such a manner that the channels remain in the closed configuration during toxin equilibrium. A second caveat to assigning an equivalent electrical distance to a particular residue is that we do not know to what extent, if any, permeant ions can affect our electrical distance of block measurements. If guanidinium toxins block Na channels in a "pore-directed binding event" analogous to charybdotoxin block of *Shaker* K channels (Goldstein and Miller, 1993), then we must also consider whether permeant ions influence our measurement of δ. If the Na and toxin sites overlap and Na competes with toxin binding, then hyperpolarization would also drive more Na ions into the channel and we would expect a decreased apparent affinity of toxin. This scenario would result in a small underestimate of the calculated electrical distance of block. The simplest explanation, in the context of the mutagenesis data, is that our electrical distance measurements approximate the extent of the transmembrane potential drop in the channel

at the location of the cysteine of RH1, or the phenylalanine in the analogous position (in IS5-S6) of the Br2a channel.

The voltage dependence of block by protons and divalent ions was measured when the channel was blocked in the open conformation. In contrast, the toxin voltage dependence was that of the closed channel. The similar fraction of the field sensed by the two types of blocking reactions implies that the field at this site is similar during channel gating from closed to open configurations. An important implication of the similarity in electrical distance for both conducting and nonconducting states is that this site must be continuously accessible from the outside in both closed and open channels. The common toxin/divalent site is restricted only in the sense that a potential drop occurs between the site and the extracellular milieu. In conclusion, the contradiction of voltage dependence of divalent ion block and voltage independence of toxin block is resolved by these studies, and the hypothesis that the toxin blocking site is in the ion conducting path is supported.

We thank Drs. William Green, Jonathan Makielski, and Dorothy Hanck for helpful discussions and reading of this manuscript. Dr. Al. Goldin (UC-Irvine) kindly provided us with the Br2a clone.

This work was supported by National Institutes of Health grant PO1-HL20592 and grants-in-aid form the American Heart Association Metropolitan Chicago Affiliate.

REFERENCES

Backx, P., D. Yue, J. Lawrence, E. Marban, and G. Tomaselli. 1992. Molecular localization of an ion-binding site within the pore of mammalian sodium channels. *Science*. 257:248–251.

Carmeliet, E. 1987. Voltage-dependent block by tetrodotoxin of the sodium channel in rabbit cardiac Purkinje fibers. *Biophys. J* 51:109–114.

Cohen, C. J., B. P. Bean, T. J. Colatsky, and R. W. Tsien. 1981. Tetrodotoxin block of sodium channels in rabbit Purkinje fibers: interactions between toxin binding and channel gating. *J. Gen. Physiol.* 78:383–411.

Cole, K. S., and J. W. Moore. 1960. Potassium ion current in the squid giant axon: dynamic characteristics. *Biophys. J.* 1:161–202.

Daumas, P., and O. S. Andersen. 1993. Proton block of rat brain sodium channels: evidence for two proton binding sites and multiple occupancy. *J. Gen. Physiol.* 101:27–43.

Doyle, D. D., Y. G. Guo, S. L. Lustig, J. Satin, R. B. Rogart, and H. A. Fozzard. 1993. Divalent cation competition with ^{3}H-saxitoxin binding to tetrodotoxin-resistant and -sensitive sodium channels. A two-site structural model of ion/toxin interaction. *J. Gen. Physiol.* 101:153–182.

Eickhorn, R., J. Weirich, D. Hornung, and H. Antoni. 1990. Use dependence of sodium current inhibition by tetrodotoxin in rat cardiac muscle: influence of channel state. *Pflügers Arch.* 416:398–405.

French, R. J., J. F. Worley, and B. K. Krueger. 1984. Voltage-dependent block by saxitoxin of sodium channels incorporated into planar lipid bilayers. *Biophys. J.* 45:301–310.

Goldstein, S. A. N., and C. Miller. 1993. Mechanism of charybdotoxin block of a voltage-gated K channel. *Biophys. J.* 65:1613–1619.

Green, W. N., L. B. Weiss, and O. S. Andersen. 1987a. Batrachotoxin-modified sodium channels in planar lipid bilayers: characterization of saxitoxin- and tetrodotoxin-induced channel closures. *J. Gen. Physiol.* 89:873–903.

Green, W. N., L. B. Weiss, and O. S. Andersen. 1987b. Batrachotoxin-modified sodium channels in planar lipid bilayers: ion permeation and block. *J. Gen. Physiol.* 89:841–872.

Guo, Z., A. Uehara, A. Ravindran, S. H. Bryant, S. Hall, and E. Moczydlowski. 1987. Kinetic basis for insensitivity to tetrodotoxin and saxitoxin in sodium channels of canine heart and denervated rat skeletal muscle. *Biochemistry*. 26:7346–7556.

Guy, H. R., and F. Conti. 1990. Pursuing the structure and function of voltage-gated channels. *TINS*. 13:201–206.

Heinemann, S. H., H. Terlau, and K. Imoto. 1992. Molecular basis for pharmacological differences between brain and cardiac sodium channels. *Pflugers Arch.* 422:90–92.

Hille, B. 1975. The receptor for tetrodotoxin and saxitoxin. A structural hypothesis. *Biophys. J.* 15:615–619.

Hille, B. 1992. Ionic Channels of Excitable Membranes. Vols. 3–4. 2nd Ed. Sinauer Associates, Sunderland, MA. 607 pp.

Isom, L. L., K. S. Dejongh, D. E. Patton, B. F. X. Reber, J. Offord, H. Charbonneau, K. Walsh, A. L. Goldin, and W. A. Catterall. 1992. Primary structure and functional expression of the beta1-subunit of the rat brain sodium channel. *Science* 256:839–842.

Krueger, B. K., J. F. Worley, and R. J. French. 1986. Block of sodium channels in planar lipid bilayers by guanidinium toxins and calcium: are the mechanism of voltage dependence the same? *In* Tetrodotoxin, Saxitoxin, and the Molecular Biology of the Sodium Channel, C. Y. Kao and S. R. Levinson, editors. New York Academy of Sciences, New York. 257–268.

Lönnendonker, U. 1989. Use-dependent block of sodium channels in frog myelinated nerve by tetrodotoxin and saxitoxin at negative holding potentials. *Biochim. Biophys. Acta.* 985:153–160.

Makielski, J. C., J. Satin, and Z. Fan. 1993. Post-repolarization block of cardiac sodium channels by saxitoxin. *Biophys. J.* 65:790–798.

Moczydlowski, E., S. Hall, S. S. Garber, G. S. Strichartz, and C. Miller. 1984. Voltage-dependent blockade of muscle Na^+ channels by Guanidinium toxins. *J. Gen. Physiol.* 84:687–704.

Nilius, B. 1988. Calcium block of guinea-pig heart sodium channels with and without modification by the piperazinylindole DPI 201–106. *J. Physiol.* 399:537–558.

Noda, M., H. Suzuki, S. Numa, and W. Stühmer. 1989. A single point mutation confers tetrodotoxin and saxitoxin insensitivity on the sodium channel-II. *FEBS Lett.* 259:213–216.

Patton, D. E., and A. L. Goldin. 1991. A voltage-dependent gating transition induces use-dependent block by tetrodotoxin of rat IIA sodium channels expressed in Xenopus oocytes. *Neuron.* 7:637–647.

Rando, T. A., and G. R. Strichartz. 1986. Saxitoxin blocks batrachotoxin-modified sodium channels in the node of Ranvier in a voltage-dependent manner. *Biophys. J.* 49:785–794.

Ravindran, A., L. Schild, and E. Moczydlowski. 1991. Divalent cation selectivity for external block of voltage-dependent Na^+ channels prolonged by batrachotoxin—Zn^{2+} induces discrete substates in cardiac Na^+ channels. *J. Gen. Physiol.* 97:89–115.

Salgado, V. L., J. Z. Yeh, and T. Narahashi. 1986. Use- and voltage-dependent block of the sodium channel by saxitoxin. *In* Tetrodotoxin, Saxitoxin and the Molecular Biology of the Sodium Channel. Vol. 479. C. Y. Kao and S. R. Levinson, editors. The New York Academy of Sciences, New York. 84–95.

Satin, J., J. W. Kyle, M. Chen, P. Bell, L. L. Cribbs, H. A. Fozzard, and R. B. Rogart. 1992a. A mutant of TTX-resistant cardiac sodium channels with TTX-sensitive properties. *Science*. 256:1202–1205.

Satin, J., J. W. Kyle, M. Chen, R. B. Rogart, and H. A. Fozzard. 1992b. The cloned cardiac sodium channel α-subunit expressed in Xenopus oocytes show gating and blocking properties of native channels. *J. Membr. Biol.* 130:11–22.

Satin, J. C., J. W. Kyle, R. B. Rogart, H. A. Fozzard, and J. C. Makielski. 1994. Post-repolarization block of cloned sodium channels by saxitoxin; the contribution of pore-region amino acids. *Biophys. J.* 66: 1353–1363.

Schild, L., and E. Moczydlowski. 1991. Competitive binding interaction between Zn^{2+} and saxitoxin in cardiac Na^+ channels—evidence for a sulfhydryl group in the Zn^{2+} saxitoxin binding site. *Biophys. J.* 59:523–537.

Sheets, M. F., and D. A. Hanck. 1992. Mechanisms of extracellular divalent and trivalent block of the sodium current in canine cardiac Purkinje cells. *J. Physiol.* 454:299–320.

Sheets, M. F., B. E. Scanley, D. A. Hanck, J. C. Makielski, and H. A. Fozzard. 1987. Open sodium channel properties of single canine cardiac Purkinje cells. *Biophys. J.* 52:13–22.

Taylor, R. E., and F. Bezanilla. 1983. Sodium and gating current time shifts resulting from changes in initial conditions. *J. Gen. Physiol.* 81:773–784.

Terlau, H., S. H. Heinemann, W. Stuhmer, M. Pusch, F. Conti, K. Imoto, and S. Numa. 1991. Mapping the site of block by tetrodotoxin and saxitoxin of sodium channel-II. *FEBS Lett.* 293:93–96.

Ulbricht, W., H. H. Wagner, and J. Schmidtmayer. 1986. Kinetics of TTX-STX block of sodium channels. *In* Tetrodotoxin, Saxitoxin and the Molecular Biology of the Sodium Channel. New York Academy of Sciences. Vol. 479. C. Y. Kao and S. R. Levinson, editors. 68–83.

Vassilev, P. M., R. W. Hadley, K. S. Lee, and J. R. Hume. 1986. Voltage-dependent action of tetrodotoxin in mammalian cardiacmyocytes. *Am. J. Physiol.* 251:H475–H480.

Woodhull, A. M. 1973. Ionic blockage of sodium channels in nerve. *J. Gen. Physiol.* 61:687–708.

Worley, J. F. I. I. I., and B. K. Krueger. 1984. Voltage-dependent block by saxitoxin of sodium channels incorporated into planar lipid bilayers. *Biophys. J.* 45:301–310.

Yamamoto, D., J. Z. Yeh, and T. Narahashi. 1984. Voltage-dependent calcium block of normal and tetramethrin-modified single sodium channels. *Biophys. J.* 45:337–344.